ICSV14
Cairns • Australia
9-12 July, 2007

14th International Congress on Sound & Vibration

THE EFFECT OF BOUNDARY CONDITIONS ON ACTIVE CONTROL OF SOUND RADIATION FROM A RECTANGULAR PLATE

Jingtao Du, Guoyong Jin, Tiejun Yang , Zhigang Liu, Wanyou Li

College of Power and Energy Engineering, Harbin Engineering University,
Harbin, 150001, P. R. China
jingtaodu828@yahoo.com.cn

Abstract

This paper deals with the active control of sound radiation from a rectangular plate with general boundary condition. A baffled rectangular plate with elastic boundary restraints is subjected to a steady-state harmonic point force, and the resulting radiated sound field is minimized by applying point forces as control input. Modal parameters are obtained by employing an improved Fourier series method (IFSM) to construct a set of admissible functions for the Rayleigh-Ritz procedure. In conjunction with this method, vibration response is derived utilizing modal superposition theory. Velocity mobility curves from such method with those of analytical solutions for simply supported boundary case are compared. The agreements are excellent. The optimized control force is then calculated for global attenuation based on this model. The effects of boundary conditions on active control are shown and discussed through computer simulations mainly performed for two special cases.

1. INTRODUCTION

In recent years, considerable research has been devoted to active control of sound radiation from plate structure by means of structural control, known as active structural acoustic control (ASAC). Majority of the published work has been confined to the plate structure with classical boundary conditions, i.e. simply supported or clamped supported boundary conditions [1-3]. However, in practice, the types of the edge conditions are not just limited to above two types, and little work has been done on studying how the boundary conditions will affect control performance.

In this paper, active control of sound radiation from a baffled elastically restrained plate is considered. The modal analysis of the plate with homogeneous elastic supports along the edges is performed by using an improved Fourier series method (IFSM), recently proposed by Li [4], to construct a set of admissible functions in the Rayleigh-Ritz procedure. Modal superposition method is then employed to derive the plate vibration response to point force. Based on this plate model developed, two special types of edge spring stiffness variation are mainly taken as examples to show the effect of boundary conditions on the control results of active control of sound radiation.

2. VIBRATION RESPONSE OF ELASTICALLY RESTRAINED PLATE

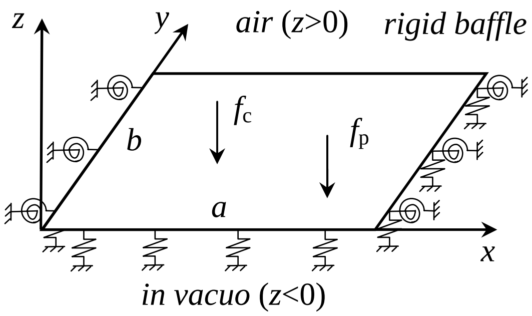

Figure 1. Elastically restrained plate model and co-ordinate system

A vibrating elastically restrained rectangular plate located in an infinite baffle radiates sound into the upper semi-infinite space, as Fig. 1 illustrated. The surface velocity distribution as the input of sound radiation can be written in terms of the structural mobility Y such that

$$\upsilon = Yf \tag{1}$$

where f is the steady-state harmonic point force applied onto the structure surface in the normal direction. The structural mobility in the above equation can be written out according to modal superposition theory as

$$Y = \sum_{n=1}^{N} \frac{j\omega\varphi_n(x_f, y_f)\varphi_n(x, y)}{m_n(\omega_n^2 + 2j\xi\omega_n\omega - \omega^2)} \tag{2}$$

where ω_n and φ_n are the natural angular frequency and mode shape distribution function of the *nth* structural mode, respectively; n is the mode order number, N is the total mode number considered in the modal superposition. ω is the angular frequency of excitation; (x_f, y_f) and (x, y) denote the locations of the point force application and response point on the surface of plate, respectively. ξ is the modal damping ratio; m_n is the modal mass defined as

$$m_n = \int_0^a \int_0^b \rho h \varphi_n^2(x, y) dxdy \tag{3}$$

where ρ is the mass density of plate material, h is the plate thickness.

Following Li’s work [5], the modal characteristic parameters of rectangular plate with general boundary conditions can be obtained by suing an improved Fourier series method to select a set of admissible functions in the Rayleigh-Ritz procedure. For a purely bending plate, the total potential energy can be derived as follows

$$V_{\max} = \frac{D}{2}\int_0^a\int_0^b \left\{ \left(\frac{\partial^2 w}{\partial x^2}\right)^2 + \left(\frac{\partial^2 w}{\partial y^2}\right)^2 + 2\nu \frac{\partial^2 w}{\partial x^2}\frac{\partial^2 w}{\partial y^2} + 2(1-\nu)\left(\frac{\partial^2 w}{\partial x \partial y}\right)^2 \right\} dxdy$$
$$+\frac{1}{2}\int_0^b \left[k_{x0} w^2 + K_{x0}\left(\frac{\partial w}{\partial x}\right)^2 \right]_{x=0} dy + \frac{1}{2}\int_0^b \left[k_{x1} w^2 + K_{x1}\left(\frac{\partial w}{\partial x}\right)^2 \right]_{x=a} dy \qquad (4)$$
$$+\frac{1}{2}\int_0^a \left[k_{y0} w^2 + K_{y0}\left(\frac{\partial w}{\partial y}\right)^2 \right]_{y=0} dx + \frac{1}{2}\int_0^a \left[k_{y1} w^2 + K_{y1}\left(\frac{\partial w}{\partial y}\right)^2 \right]_{y=b} dx$$

where D, w, and ν are, respectively, flexural rigidity, flexural displacement of plate, and Poisson’s ratio of the panel. k is the translational edge spring constant, and K is the rotational edge spring constant, respectively. The subscripts with k and K indicate the location of the corresponding boundary springs. For example, k_{x0} presents the stiffness of the translational edge spring at x=0. Any types of classical boundary conditions can be easily obtained by setting the boundary spring stiffness into infinite or zero.
The total kinetic energy is calculated from

$$T_{\max} = \frac{1}{2}\int_0^a\int_0^b \rho h \left(\frac{\partial w}{\partial t}\right)^2 dxdy \qquad (5)$$

An improved Fourier series method has been recently proposed for the vibration analysis of generally supported beams [4]. The flexural displacement of the beam is sought as the linear combination of Fourier series and an auxiliary polynomial function

$$\psi_m(x) = \sum_{m=0}^{\infty} a_m \cos\lambda_{am} x + p(x) \quad \left(\lambda_{am} = m\pi / a\right), \quad 0 \le x \le a \qquad (6)$$

Here, the function $p(x)$ is introduced to take care of the potential discontinuities of the original displacement function and its derivatives at the end points.

For plate problems, the products of the beam functions are often chosen as the admissible functions and the displacement function can be accordingly expressed as

$$w(x,y) = \sum_{m,n=0}^{\infty} A_{mn}\psi_m^a(x)\psi_n^b(y) \qquad (7)$$

Here, A_{mn} are the unknown coefficients to be determined in the Rayleigh-Ritz procedure. Substituting Eq. (7) into Eqs. (4) and (5), and minimizing the Rayleigh quotient with respect to the undetermined coefficients

$$\frac{\partial}{\partial A_{mn}}(V_{\max} - T_{\max}) = 0 \qquad (8)$$

When all the series expansions are numerically truncated to m=M and n=N, the matrix equation below can be finally derived

$$\left(\mathbf{K} - \rho_D \omega^2 \mathbf{M}\right)\mathbf{A} = 0 \qquad (9)$$

where $\rho_D = \rho h/D$; **K** and **M** are, respectively, stiffness matrix and mass matrix. ω is the frequency in radian. The detailed expression of the every term can be found in Ref [5]. The natural frequencies and eigenvectors can now be easily determined by solving a standard matrix eigenproblem. The mode shapes can be simply calculated using Eq. (7).

$$\phi(x,y) = \sum_{m=0}^{M}\sum_{n=0}^{N}\left(\cos\lambda_{am}x + \mathbf{X}^{\mathrm{T}}\overline{\mathbf{S}}_{am}\right)\left(\cos\lambda_{bn}y + \mathbf{Y}^{\mathrm{T}}\overline{\mathbf{S}}_{bn}\right)\overline{A}_{mn} \tag{10}$$

where

$$\mathbf{X} = \left\{1 \quad x \quad x^2 \quad x^3 \quad x^4\right\}^{\mathrm{T}}, \qquad \overline{\mathbf{S}}_{am} = \mathbf{L}_a\mathbf{H}_a^{-1}\mathbf{Q}_{am} \tag{11-a,b}$$

$$\mathbf{L}_a = \begin{bmatrix} \frac{8a^3}{360} & \frac{7a^3}{360} & -\frac{a}{3} & -\frac{a}{6} \\ 0 & 0 & 1 & 0 \\ -\frac{a}{6} & -\frac{a}{12} & -\frac{1}{2a} & \frac{1}{2a} \\ \frac{1}{6} & 0 & 0 & 0 \\ -\frac{1}{24a} & \frac{1}{24a} & 0 & 0 \end{bmatrix}, \quad \mathbf{H}_a = \begin{bmatrix} \frac{8\hat{k}_0a^3}{360}+1 & \frac{7\hat{k}_0a^3}{360} & \frac{-\hat{k}_0a}{3} & \frac{-\hat{k}_0a}{6} \\ \frac{7\hat{k}_1a^3}{360} & \frac{8\hat{k}_1a^3}{360}+1 & \frac{-\hat{k}_1a}{6} & \frac{-\hat{k}_1a}{3} \\ \frac{a}{3} & \frac{a}{6} & \widehat{K}_0+\frac{1}{a} & \frac{-1}{a} \\ \frac{a}{6} & \frac{a}{3} & \frac{-1}{a} & \widehat{K}_1+\frac{1}{a} \end{bmatrix} \tag{12-a, b}$$

and $$\mathbf{Q}_{am} = \left\{-\hat{k}_0 \quad (-1)^m\hat{k}_1 \quad -\lambda_{am}^2 \quad (-1)^m\lambda_{am}^2\right\}^{\mathrm{T}}. \tag{13}$$

The counterparts in y-direction can be readily written out by simply replacing a and m in the above expressions with b and n, respectively. Making use of the equation

$$\int_0^a\int_0^b \phi^2 dxdy = ab \tag{14}$$

The normalizing factor can be determined by the following equation

$$\begin{aligned}
\eta^2 &= \frac{1}{ab}\int_0^a\int_0^b\left[\sum_{m,n=0}\left(\cos\lambda_{am}x + \mathbf{X}^{\mathrm{T}}\overline{\mathbf{S}}_{am}\right)\left(\cos\lambda_{bn}y + \mathbf{Y}^{\mathrm{T}}\overline{\mathbf{S}}_{bn}\right)\right] \\
&\left[\sum_{m',n'=0}\left(\cos\lambda_{am'}x + \mathbf{X}^{\mathrm{T}}\overline{\mathbf{S}}_{am'}\right)\left(\cos\lambda_{bn'}y + \mathbf{Y}^{\mathrm{T}}\overline{\mathbf{S}}_{bn'}\right)\right]dxdy \\
&= \frac{1}{ab}\int_0^a\int_0^b\sum_{m,n=0}\left(\cos\lambda_{am}x\cos\lambda_{bn}y + \cos\lambda_{am}x\mathbf{Y}^{\mathrm{T}}\overline{\mathbf{S}}_{bn} + \mathbf{X}^{\mathrm{T}}\overline{\mathbf{S}}_{am}\cos\lambda_{bn}y + \mathbf{X}^{\mathrm{T}}\overline{\mathbf{S}}_{am}\mathbf{Y}^{\mathrm{T}}\overline{\mathbf{S}}_{bn}\right) \\
&\sum_{m',n'=0}\left(\cos\lambda_{am'}x\cos\lambda_{bn'}y + \cos\lambda_{am'}x\mathbf{Y}^{\mathrm{T}}\overline{\mathbf{S}}_{bn'} + \mathbf{X}^{\mathrm{T}}\overline{\mathbf{S}}_{am'}\cos\lambda_{bn'}y + \mathbf{X}^{\mathrm{T}}\overline{\mathbf{S}}_{am'}\mathbf{Y}^{\mathrm{T}}\overline{\mathbf{S}}_{bn'}\right)dxdy \\
&= \sum_{m,n=0}\sum_{m',n'=0}\left[\delta(m,m')\delta(n,n') + \delta(m,m')\mathbf{C}_{bn}^{\mathrm{T}}\overline{\mathbf{S}}_{bn'} + \mathbf{C}_{am}^{\mathrm{T}}\overline{\mathbf{S}}_{am'}\delta(n,n')\right. \\
&+\mathbf{C}_{am}^{\mathrm{T}}\overline{\mathbf{S}}_{am'}\mathbf{C}_{bn}^{\mathrm{T}}\overline{\mathbf{S}}_{bn'} + \delta(m,m')\mathbf{C}_{bn'}^{\mathrm{T}}\overline{\mathbf{S}}_{bn} + \delta(m,m')\overline{\mathbf{S}}_{bn}^{\mathrm{T}}\overline{\mathbf{Y}}\overline{\mathbf{S}}_{bn'} + \mathbf{C}_{am}^{\mathrm{T}}\overline{\mathbf{S}}_{am'}\mathbf{C}_{bn'}^{\mathrm{T}}\overline{\mathbf{S}}_{bn} \\
&+\mathbf{C}_{am}^{\mathrm{T}}\overline{\mathbf{S}}_{am'}\overline{\mathbf{S}}_{bn}^{\mathrm{T}}\overline{\mathbf{Y}}\overline{\mathbf{S}}_{bn'} + \mathbf{C}_{am'}^{\mathrm{T}}\overline{\mathbf{S}}_{am}\delta(n,n') + \mathbf{C}_{am'}^{\mathrm{T}}\overline{\mathbf{S}}_{am}\mathbf{C}_{bn}^{\mathrm{T}}\overline{\mathbf{S}}_{bn'} + \overline{\mathbf{S}}_{am}\overline{\mathbf{X}}\overline{\mathbf{S}}_{am'}\delta(n,n') \\
&+\overline{\mathbf{S}}_{am}\overline{\mathbf{X}}\overline{\mathbf{S}}_{am'}\mathbf{C}_{bn}^{\mathrm{T}}\overline{\mathbf{S}}_{bn'} + \mathbf{C}_{am'}^{\mathrm{T}}\overline{\mathbf{S}}_{am}\mathbf{C}_{bn'}^{\mathrm{T}}\overline{\mathbf{S}}_{bn} + \mathbf{C}_{am'}^{\mathrm{T}}\overline{\mathbf{S}}_{am}\overline{\mathbf{S}}_{bn}^{\mathrm{T}}\overline{\mathbf{Y}}\overline{\mathbf{S}}_{bn'} + \overline{\mathbf{S}}_{am}^{\mathrm{T}}\overline{\mathbf{X}}\overline{\mathbf{S}}_{am'}\mathbf{C}_{bn'}^{\mathrm{T}}\overline{\mathbf{S}}_{bn} \\
&\left.+\overline{\mathbf{S}}_{am}^{\mathrm{T}}\overline{\mathbf{X}}\overline{\mathbf{S}}_{am'}\overline{\mathbf{S}}_{bn}^{\mathrm{T}}\overline{\mathbf{Y}}\overline{\mathbf{S}}_{bn'}\right]A_{mn}A_{m'n'}
\end{aligned} \tag{15}$$

Here, δ is the Kronecher delta function, and the expressions of $\overline{\mathbf{X}}$ and $\mathbf{C}$ are the same as those in Ref. [4].
The normalized mode shape coefficients in Eq. (10) can be written as

$$\overline{A}_{mn} = A_{mn} / \eta \tag{16}$$

Submitting the normalized mode shape into Eq. (2), the structural mobility function can be rewritten as follows

$$Y = \sum_{n=1}^{N} \frac{j\omega\phi_n(x_f, y_f)\phi_n(x, y)}{\rho hab(\omega_n^2 + 2j\xi\omega_n\omega - \omega^2)} \tag{17}$$

3. RADIATED SOUND POWER AND GLOBAL CONTROL

The radiated sound power can be easily calculated by the velocity distributions with no need to explicitly calculate the far-field sound pressure. This formulation of sound radiated power can be expressed in terms of the contributions of the velocity of a number of individually radiating elements of the plate surface [6]

$$W = \mathbf{v}^{\mathrm{H}}\mathbf{R}\mathbf{v} \tag{18}$$

where $\mathbf{R}$ is the radiation resistance matrix. For the case in which the radiating surface is plane and in an infinite baffle, the terms of this radiation resistance matrix can be calculated analytically. And the superscript **H** denotes the Hermitian transpose.

The cost function that the control system seeks to minimize will be the total radiated sound power. The total response of the plate $\mathbf{v}_{\mathrm{tot}}$ will be a superposition of two parts: the vibration due to the primary point force f_{p} and the vibration due to the control point force f_{c}.

$$\mathbf{v}_{tot} = \mathbf{Y}_p f_p + \mathbf{Y}_c f_c \tag{19}$$

Substituting the velocity into the equation for sound power radiation, equation (18), the radiated sound power, W, gives:

$$W = f_c^{\mathrm{H}}\mathbf{Y}_c^{\mathrm{H}}\mathbf{R}\mathbf{Y}_c f_c + f_c^{\mathrm{H}}\mathbf{Y}_c^{\mathrm{H}}\mathbf{R}\mathbf{Y}_p f_p + f_p^{\mathrm{H}}\mathbf{Y}_p^{\mathrm{H}}\mathbf{R}\mathbf{Y}_c f_c + f_p^{\mathrm{H}}\mathbf{Y}_p^{\mathrm{H}}\mathbf{R}\mathbf{Y}_p f_p \tag{20}$$

This equation is of standard Hermitian quadratic form. Since $\mathbf{R}$ is positive definite, the cost function of W has a unique minimum value. And the optimum control force that minimizes the total sound power is

$$f_{c,opt} = -(\mathbf{Y}_c^{\mathrm{H}}\mathbf{R}\mathbf{Y}_c)^{-1}(\mathbf{Y}_c^{\mathrm{H}}\mathbf{R}\mathbf{Y}_P f_p) \tag{21}$$

The resulting minimum achievable sound power output for the particular control source arrangement can be derived by substituting Eq. (21) into Eq. (20).

4. NUMERICAL SIMULATION AND DISCUSSION

The results of computer simulations for the active control of sound radiation from a rectangular plate with general boundary conditions will be presented. The rectangular plate parameters are given in Table 1. The damping ratio of ξ=0.002 was utilized for all mode cases. It was assumed that the plate was radiating into the air in this study. Firstly, to evaluate the prediction accuracy of the current plate model, two velocity mobility curves obtained from this model are compared with those of analytical solutions under the simply supported boundary condition case. These two comparison curves are given in Figs. 2 and 3, the application location of the primary point force is (0.37, 0.1), and the response point location for calculation of transfer mobility is (0.2, 0.22).

Table 1. Rectangular plate parameters.

Parameter	Value
length, a (m)	0.42
width, b (m)	0.28
thickness, h (mm)	1.8
Young's modulus, E (GPa)	71
density, ρ (kg/m^3)	2720
Poisson's ratio, v	0.33

The truncated numbers of terms M=N=6 are used in the calculation. It can be found that this model can predict the structural response with excellent accuracy.

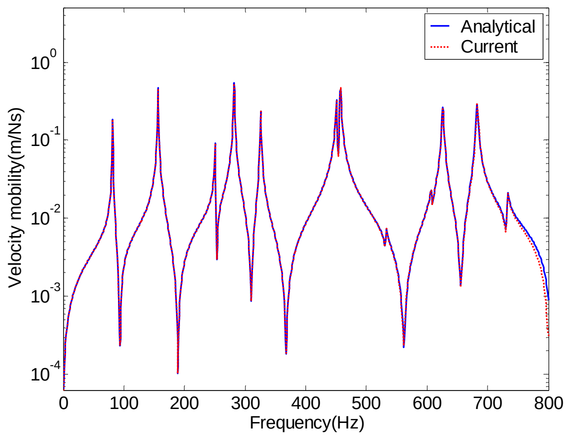

Figure 2. Comparison of driving point mobility

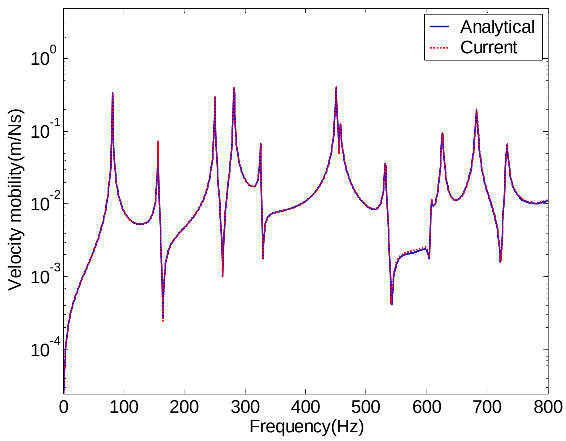

Figure 3. Comparison of transfer point mobility

Now, let us use this model to study the effect of boundary conditions on the active control of sound radiation by applying a secondary control point force, applied at location of (0.18, 0.12) on this plate surface. The complex amplitude of the primary point force is 1 N in the simulation. It is assumed that the four edges have the same uniform edge spring stiffness. The translational and rotational spring stiffness constants are denoted by using k_t and K_r, respectively. For the sake of the simplification, two special cases are considered. One case is that a simply supported plate with uniform rotational spring stiffness along each edge. The other is that the translational edge spring stiffness varies while the rotational spring stiffness is infinitely large. Both the attenuation and sound power after control are compared to demonstrate the effect of the boundary conditions on active structural acoustic control. The reference value 10^{-12} W is used for the calculation of radiated sound power dB value.

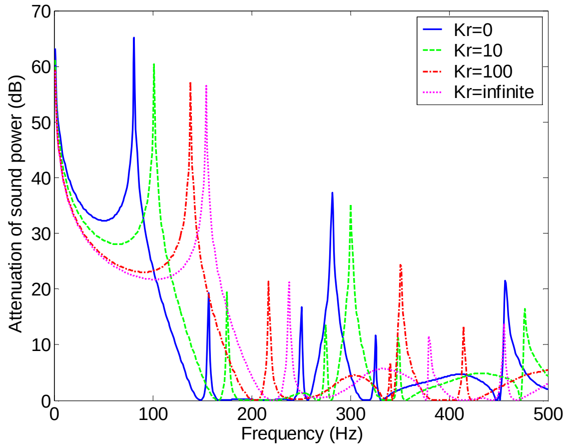

Figure 4. Attenuation of radiated sound power with variation of K_r

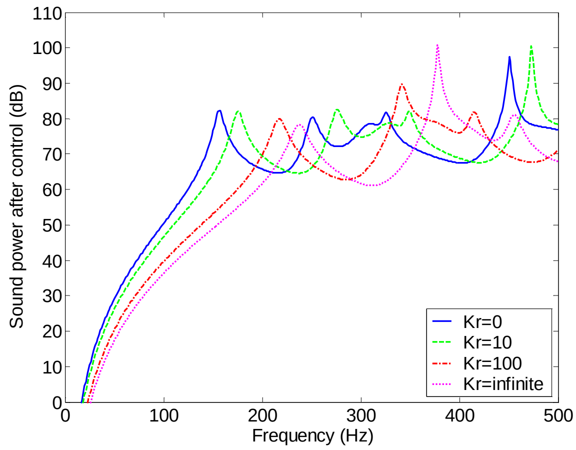

Figure 5. Radiated sound power after control with variation of K_r

The first case we consider is a simply supported rectangular plate with elastic restraints against edge rotations. The effect results under different rotational spring stiffness are shown in Figs. 4 and 5. Active control is effective for each case shown in the two Figs above. At very low frequency, the purely simply supported case has the biggest attenuation of sound power. With the rotation restraint further increasing, the peaks of the active control attenuation are shifted toward higher frequency. The speed of the effect is rapid when rotational spring stiffness is relatively small. By comparing Fig. 4 with Fig. 5, it can be found that the variation trend of attenuation of sound power is not coincident with the final control results for the same control configuration. Case of $K_r = \infty$ is corresponded to the clamped supported boundary condition. It has the best control result at the low frequency. Increase of the rotational stiffness can improved low frequency control result aiming at the minimization of radiated sound power.

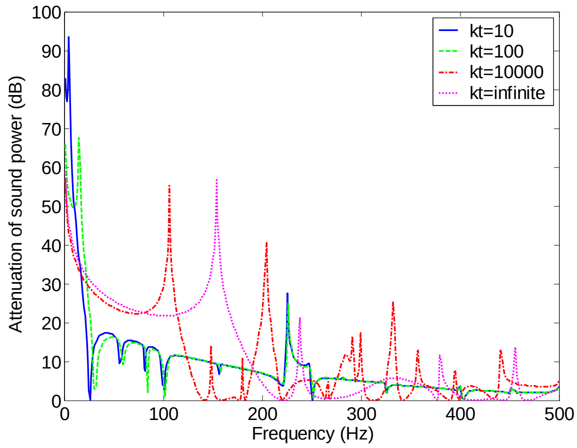

Figure 6. Attenuation of radiated sound power with variation of k_t

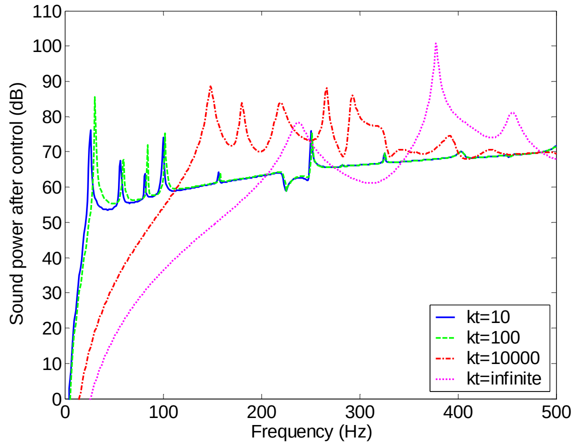

Figure 7. Radiated sound power after control with variation of k_t

For the second case considered in this simulation, the translation spring stiffness varies from 10 to infinite, while setting K_r into infinite for each case. The simulation results are provided in Figs. 6 and 7. It can be found that this type of edge spring has opposite effect trend compared with that of the translation type. For the case in which the translation spring is very soft, the active control has little effectiveness on the sound radiation control except the extremely low fundamental frequency. When the value of k_t varies in very small value range, the variation of control performance is not obvious. With the further increase of k_t, the control performance is gradually improved in the low frequency range.

5. CONCLUSIONS

An analytical model for predicting the active control performance of sound power radiated by an elastically restrained rectangular plate along the edges, by application of secondary point control force, has been developed. The accuracy of this model has been demonstrated by comparison of velocity mobility curves with the analytical results under the simply supported boundary condition. Both of agreements are excellent. This model is generally applicable to investigate the effect of elastic restraint along any edge on the active control of sound radiation from a rectangular plate.

In the first case studied in this paper, the trend of attenuation is opposite with that of the control result at the low frequency, which suggests that the boundary condition play an important role for the active control. It should be seriously considered to design the active system aiming at the best control effectiveness. Interesting phenomenon has been found in the second case where the variation of the translation stiffness is considered with the rotational stiffness $K_r = \infty$ that the active control is not effective for the little translational stiffness case. With the increase of k_t, control performance will be gradually improved during the low frequency range. These two cases here show different effect of boundary conditions on the active control. So as to achieve the best control performance, the boundary condition effect should be taken into consideration during the system design and further study will be carried out to discover this effect more in depth.

REFERENCES

[1] C. R. Fuller, "Active control of sound transmission/radiation from elastic plates by vibration inputs: I. analysis", *Journal of Sound and Vibration* **136**, 1-15 (1990).

[2] Jie Pan, Scott D. Snyder and Colin H. Hansen, "Active control of far-field sound radiated by a rectangular panel-A general analysis", *Journal of the Acoustical Society of America* **91**, 2056-2066 (1992).

[3] C. C. Sung and C. Y. Chiu, "Control of sound transmission through thin plate", *Journal of Sound and Vibration* **218**, 605-618 (1998).

[4] W. L. Li, "Free vibrations of beams with general boundary conditions", *Journal of Sound and Vibration* **237**, 709-725 (2000).

[5] W. L. Li, "Vibration analysis of rectangular plates with general elastic boundary supports", *Journal of Sound and Vibration* **273**, 619-635 (2004).

[6] S. J. Elliott and M. E. Johnson, "Radiation modes and the active control of sound power", *Journal of the Acoustical Society of America* **94**, 2194-2204 (1993).